Master thesis 2020

Department of Mathematical Sciences and Technology

Supplying an off-grid charging station for the Thorvald Agricultural Robot with energy using PV-technology

Silje Sæbø Dale

Mechanical Engrineering

Preface

For this project I was set out research the possibilities of energy supply for a charging station for the Thorvald robots. In this process I would like to than my supervisor Lars Grimstad for discussions and guidance. A workshop at PUC-Rio contributed to my understanding of agricultural robots and sparked my enthusiasm for this topic.

I would also like to thank Guillaume for moral support, Monty for great advice and discussion, Katarina for help with "å dra det i land", and Victoria for proof reading.

Abstract

Within the field of agriculture a tremendous technological advancement is taking place, as an increasing world population needs to be fed. One of the recent technological advancements in agriculture are agricultural robots. This thesis seeks to dimension a battery bank and PV-modules needed to supply a charging station for the Thorvald agriculture robot. The charging station is situated at a strawberry farm in Coxheath, England, and supplies three Thorvald robots. Measurements of robot energy consumption has been carried out and insolation has been mapped using PVGIS in order to execute these calculations. To supply the fleet of robots, it was found that $100m^2$ of fixed PV-modules or 75 m^2 of sun tracking PV-modules, and a battery capacity of 24,4kWh is necessary to meet the set requirements for the charging station.

Sammendrag

Innen landbruksfeltet skjer en enorm teknologisk fremgang, i takt med en økende verdensbefolkning må mates. En av de nylige teknologiske fremskrittene innen landbruket er landbruksroboter. I denne oppgaven undersøkes det om det er mulig å forsyne en ladestasjon til landbruksroboten Thorvald med energi fra solceller, og hvilken dimensjon solcellene og batteribanken må være for å gjøre dette. Ladestasjonen ligger på en jordbærgård i Coxheath i England, og forsyner tre Thorvald-roboter. For å utføre disse beregningene er det foretatt målinger av robotens energiforbruk, og solinnstråling er kartlagt ved bruk av PVGIS. For å oppfylle de aktuelle kravene til ladestasjonen viste beregningene at det er behov for 100m^2 med fastmonterte PV-moduler, eller 75 m^2 bevegelige PV-moduler som følger solen, og en batterikapasitet på 24,4kWh.

List of content

Introduction

Within the field of agriculture a tremendous technological advancement is taking place, as an increasing world population needs to be fed. One of the recent technological advancements in agriculture are agricultural robots (AG). AGs are being implemented across the world to increase food production efficiency by replacing human work force, reduce the amount of pesticides by precision pesticide application, and reducing soil impact by using lightweight robots. A industrial robot is defined as a programmable multifunctional device designed to both manipulate and transport parts, tools, or specialized manufacturing implements through variable programmed paths for the performance of specific manufacturing tasks Hunt (1983). However, new technology presents new challenges and of particular importance for this thesis, is the question of supplying AR with electrical power. Thus, this thesis will examine the requirements for supplying a fleet of ARs with solar energy.

Background

The AR Thorvald developed at the University of Life Science, NMBU, is a modular robot with applications like picking strawberries and treating strawberries with UV-light to avoid the growth of mildew. The robot for UV-treatment, referred to as the UV-bot, moves a UV-light lamp through strawberry fields in either open fields or tabletop beds in polytunnels. The strawberry picking robot, referred to as the harvester, operates in polytunnels where table top beds are used for strawberry production and picks mature strawberries using sensors and machine vision.

To increase autonomy of the robot a solution is to create an off-grid charging station. An off-grid charging station is a system that consists of a power plant, an energy accumulator, a charger and the necessary electrical components for energy transmission. The goal for this system is to ensure energy self-sufficiency and minimize human interaction. To do so a power generator that is durable and low maintenance is preferable.

Scope of the thesis

The scope of this thesis is to investigate the possibility of supplying the Thorvald agriculture robot and its charging station with energy from solar panels. This thesis aims to provide calculations for the potential energy production at a farm in England. The farm is situated in Coxheath, England.

The following research questions were used to guide this study:

1. What size is required of the solar panels to produce the necessary amount of energy?
2. What size battery bank would support the charging of the Thorvald agricultural robot?

In order to calculate the required dimensions of the solar panels and battery bank, solar irradiance data was collected by using PVGIS, a science hub founded by the European Union, and measurements of battery consumption were carried out.

Theory

This chapter presents theory about solar irradiance, PV-cells, batteries, and other electrical components. The concepts explained in these sections are necessary to further understand the system designed in this study.

Solar theory

This chapter includes theory about solar radiation, geometry of the Earth and the Sun, geometry of the collector and the solar beam, atmospheric transmission, absorption and reflection, and photovoltaic power technology. The theory is based on Renewable Energy Resources by John Twidell and Tony Weir, chapter 2: Solar radiation and the greenhouse effect, unless otherwise stated (Twidell and Weir, 2015).

Solar radiation

The sun's energy stems from nuclear fusion in its core, which reaches the sun's atmosphere and heats it up to 5800 K. The radiance is then transmitted to the Earth, and the amount available outside Earth's atmosphere is defined by the solar constant, G.

$$G = 1366 \pm 2 W/m^2 \qquad (1)$$

Due to sunspots and Earth's elliptical orbit around the sun, the radiation varies between $\pm 0,3\%$ and $\pm 4\%$ respectively, but these variations do not affect a solar energy application significantly. G is therefore considered a constant.

The spectral distribution of the extra-terrestrial radiation ranges from 0,3μm to 3μm. Extra-terrestrial radiation is defined as the radiation on a plane normal to the sun, which is not affected by the atmosphere.

The total radiation at Earth's surface is the sum of radiation from a direct sun beam and the diffuse radiation. Diffuse radiation is radiation that is scattered from molecular scattering or through clouds and dust. The radiation flux through a collector plane depends on the geometry of installation and the sun.

Radiation physics

The sun is considered a black body. A black body is an object that absorbs any irradiance. Radiation from a black body is defined by Stefan-Boltzmann's law,

$$U = \sigma T^4$$

where T is the surface temperature of the body and Stefan-Boltzmann's constant is $\sigma = 5{,}67$ x 10^{-8} W/m^{2}K^4.
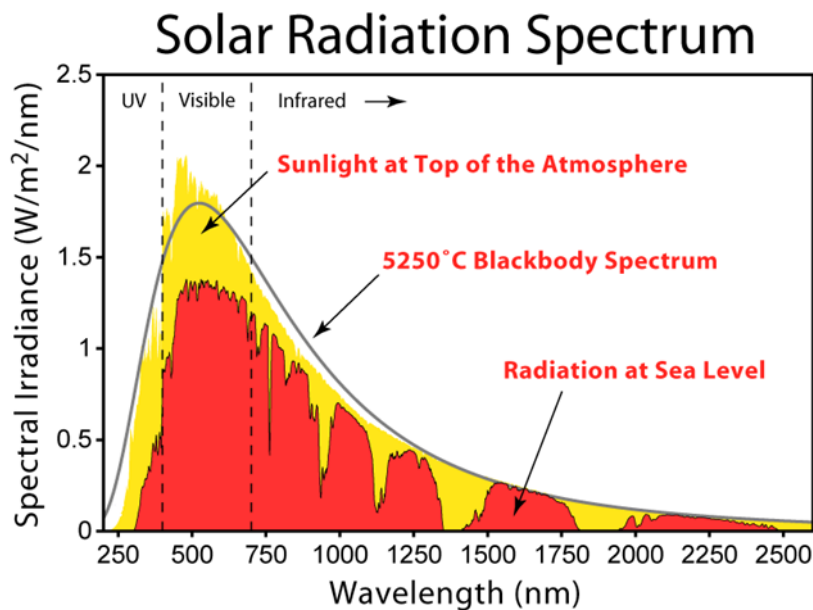
Atmospheric effects

Radiation counter interacts with Earth's atmosphere through reflection, scattering, and absorption, causing energy losses in the radiation.

Clouds, snow, and ice reflect some radiation, and this reflected radiation is called albedo. Albedo varies from place to place in the world and ranges from 0 to 1.

Molecular scattering is radiation that is spread in all directions, where some of it reaches Earth's surface and some of it radiates back towards space. There are two types of molecular scattering, Rayleigh and Mie scattering. Whereas Rayleigh scattering is caused by smaller particles and molecules in the atmosphere, Mie scattering is scattering on dust, molecules, or particles that are larger than the wavelength of the radiation.

Molecules can also absorb some energy in the radiation. Different wavelengths are absorbed by different molecules. The sun's radiation spectrum shows that radiation with wavelengths less than 400 *nm*, the UV-spectrum, are absorbed by ozone. There is little absorption in the section with visible light (400 *nm* to 700 *nm*). For radiation with wavelengths shorter than 300

nm and longer than 1200 *nm* the atmosphere does not let itself shine through. Figure 2 illustrates atmospheric effects.

REFLECTED FROM CLOUDS

SPREAD OUT

REFLECTED FROM SURFACE

ABSORBED IN
ATMOSPHERE
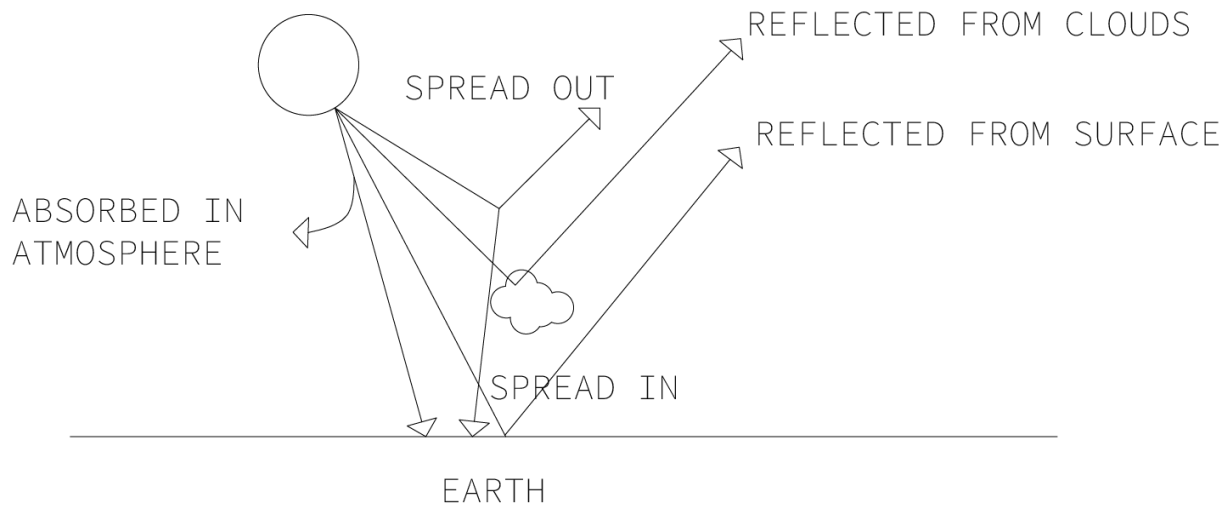
SPREAD IN

EARTH

Figure 2: Reflection, spreading and absorption of solar irradiance.

Geometry of the earth and sun

Earth rotates around its own axis, which goes through the north and the south pole. Normal to the axis is the equatorial plane. The meridional plane is parallel to the axis and normal to the equatorial plane. The amount of insolation at any point on Earth is dependent on its position, which is addressed by its latitude and longitude coordinates. Latitude is defined from the equator and is positive on the northern hemisphere and negative on the southern. Longitude is defined from the Greenwich observatory east of London.

Declination angle

The declination angle is defined as the angle between the direction of the solar radiation and the equatorial plane. Earth's rotational angle is tilted, compared to its trajectory around the sun, with an angle of $\delta_0 = 23,45^o$. The declination angle, δ, varies each day throughout the year and are at its positive and negative maximums during the summer and winter solstice, and zero at equinox. The angle can be calculated for each day during the year using the following formula,

$$\delta = \delta_0 * \sin((360°(284 + n))/365) \qquad (2)$$

where n is the day in the year, starting at $n = 1$ on January first.

Zenith angle

The zenith angle, ζ, figure 3, is the angle between a vertical line and the solar beam. Its minimum value occurs when the sun is at its highest point in the sky during the day.
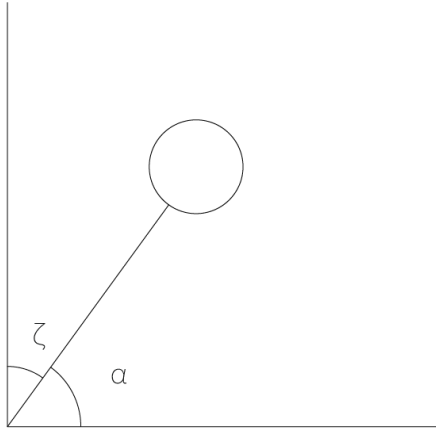

Figure 3: Zenith angle and solar altitude

Solar altitude

The solar altitude, α, is the angle between a horizontal plane and the solar beam and is complimentary to the zenith angle, shown in figure 3. The solar altitude is zero at sunrise and sunset, and at noon, local time, on the northern hemisphere, it can be calculated using the following function,

$$\alpha = 90° - \emptyset + \delta \qquad (3)$$

where $\emptyset$ it the latitude and δ is the zenith angle.

Solar time and hour angle

12 o'clock solar time refers to the time during the day where the sun is at its highest in the sky and does not depend on the actual time. Each longitude has its own solar time due to Earth's rotation, but this can deviate more than one hour from the local time during summertime.

$$local\ solar\ time\ =\ time\ +\ \frac{time\ correction}{60} \qquad (4)$$

Local solar time is calculated by correcting the time with a time correction in equation 4.

Hour angle, ω_s, converts the local solar time to the quantity of degrees the sun has moved since 12 o'clock local solar time and starts at zero.

$$\omega_s = 15°(local\ solar\ time - 12) \qquad (5)$$

The hour angle is positive after noon, and negative before noon.

Azimuth angle

The azimuth angle, A, is used to decide at which angle the solar irradiance is coming from. An illustration of the azimuth angle is shown in figure 4. The angle varies throughout the day and is also affected by latitude and time of the year. A is the angle between the solar irradiances direction and north.
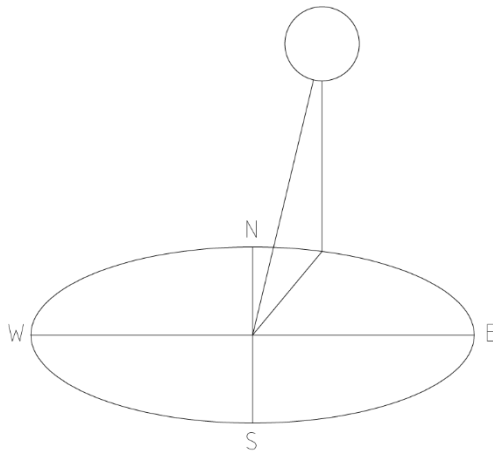
Figure 4: Azimuth angle

Air Mass

When a sun beam hits the Earth's surface, it has travelled through a certain amount of atmosphere. Depending on its angle of incidence, different ratios of air mass have been encountered by the beam. This ratio is called the air mass ratio, abbreviated as AM. Outside the atmosphere AM = 0, and AM = 1 when zenith equals zero. The definition of AM is given by the equation 6 and illustrated in figure 6.

$$AM = \frac{1}{\cos\zeta} \qquad (6)$$
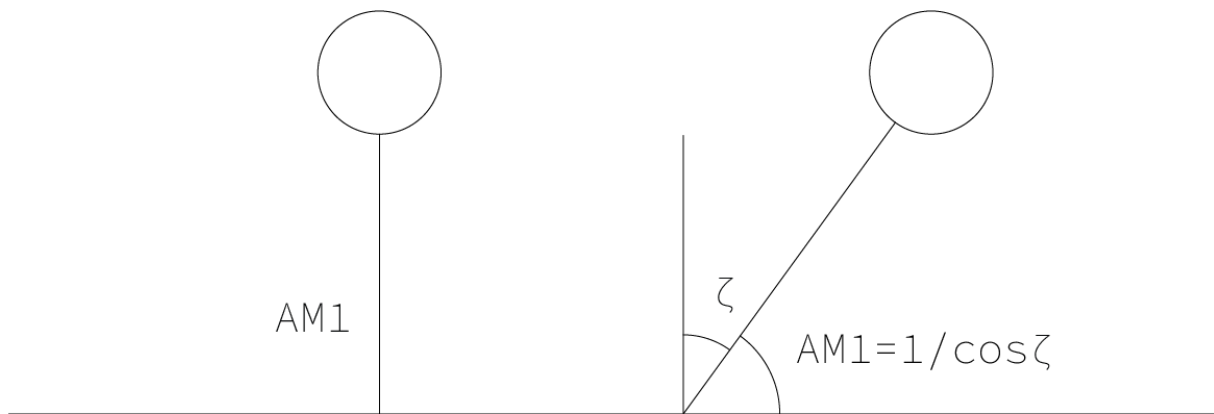
Figure 5:Airmass as AM1 and in relation to the zenith angle

Global, direct and diffuse radiation

The total radiation is comprised of direct and diffuse radiation. Direct radiation has a clear angle from the direction of the sun, and diffuse radiation comes from all directions. Diffuse radiation has been exposed to molecular scattering. The sum of direct and diffuse radiation is called the global radiation.

Inclination and orientation

The radiation from the sun, at any given location, will determine the amount of radiation a photovoltaic cell, PV-cell, receives and can be calculated by analysing the previously defined angles and equations, as well as the atmospheric. Another important parameter in determining incoming power on the PV-cell is its orientation and inclination. The radiation power at the surface of the PV-cells will be equal to the radiation from the sun if the angle of the PV-cells is 90 °, but with a fixed PV-cell, it is not possible for this to happen throughout the day because the sun moves across the sky. Fixed PV-cells that supply energy for systems that need most of their energy in winter time should be installed with a steep angle, and systems with most of their energy consumption in summertime should be installed with a "flatter" angle to optimize production in accordance with consumption. A tracking PV-plant are solar panels mounted so that they follow either one axis or two axes, so that the angle of incidence is always optimized and maximizes energy production. Tracking PV-cells are useful in locations with higher latitudes, where variations in the sun's height are larger throughout the year.

In figure 6, the inclination angle of the PV-cells, β, of the sun's height, α, and the angle of incidence are marked.
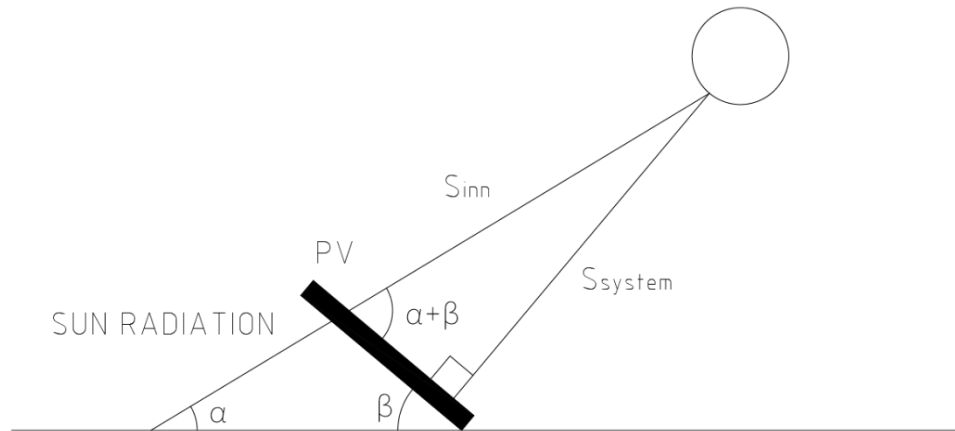

Figure 6: Radiation towards a plane of PV-cells

PV-technology

This chapter explains how electricity s generated in a photovoltaic cell and is based on Twidell and Weir's Renewable Energy Resources, chapter 5: Photovoltaic power technology (Twidell and Weir, 2015).

Solid-state physics for photovoltaics

A solar module consists of several PV-cells, and the PV-cell is where radiation from the sun is converted to electrical energy. 90% of all solar modules are made of Silisium, Si, which is a semiconductor material used in electronics. The demand for this material in the electronics industry has pushed production on pure Si. Another reason to use Si in solar panels is its bandgap. PV cells made of Si are the only technology that will be presented in this thesis.

Electricity is generated in a PV cell through the photovoltaic effect. This effect is the result of electromagnetic radiation from the sun being absorbed into a material. In this case, the radiation is considered to be photons and not waves. When a photon is absorbed, an electron is excited, and with the presence of an electric field and a closed circuit, a current is created.

The band gap model is one of the features of Si or semiconductors in general. Electrons in a semiconductor atom are in defined energy bands with different energy levels when they are in their crystal structure. When the electrons are excited from one energy level to another, they are excited from the valence band to the conduction band. The energy difference of these bands is called the band gap energy level E_g. For an electron to be excited by a photon, the

energy of the photon needs to be higher or equal to the band gap energy level of the material it is absorbed by.

$$Photon\ energy\ =\ h\nu > E_g \qquad (7)$$

The photon energy is given by the frequency of the radiation, ν, and Planck's constant, $h = 6,63 \times 10^{34}\ Js$. The band gap energy of Si is 1,11 eV and is a good fit, considering the spectrum of the sun radiation. If the energy from the photon does not excite an electron, then energy will be absorbed as heat.

When all the lowest energy levels available in an atom are occupied by electrons, it is in its ground state. The highest energy level of the ground state is called the Fermi energy, E_F, and falls in the middle of the energy levels of the valence band and the conduction band.

The ability of a semi-conductor to conduct an electron to an external circuit can be increased by adding impurities in the material. Adding impurities to the material is called doping, and by doping the material, the Fermi energy can be controlled, and the chance of exciting an electron rises. For Si, which belongs to group IV in the periodic table, one usually dopes the metal with atoms from group III or V on the periodic table.

There are two kinds of doping, n- and p-doping. n-type doping is when there are loosely bound electrons and is done by adding atoms from group V, e.g. phosphorous, in the material. This type of doping rises the Fermi level, and electrons from the added atom are more easily excited as less energy is necessary to break the bond. p-type on the other hand is doping done by adding atoms from group III and creates electron holes in the material making it easier for excited electrons to fill these holes and create a current. The Fermi level in this kind of doping is closer to the valence band.

A depletion zone is created when a n-type and p-type material are merged, also referred to as a pn-junction. The excess electrons in the n-type material will be pulled towards the holes in the n-type material, which leads to a charge displacement, and an electric field, E_p, occurs. The electric field has a positive charge near the p-type and a negative charge near the n-type material. Across the depletion zone, there will also be a potential, U. The difference in concentration of electrons leads to a diffusion current. Due to the electric field, an operating current occurs in the opposite direction.

Simply put, a solar cell is a panel of a pn-junction, with a thin layer of p-type material merged with a thicker layer of n-type material, and the widths of these are 0.25 – 0,5 μm and 150 –

200 μm, respectively. Presuming the photon energy is greater than the band gap energy, the photon travels through the p-type layer and excites an electron in the p-type layer. When the electron is excited, in the p-type material, it leaves a hole in the lattice structure and the electron is driven towards the n-type material due to the electric field. If there is an external circuit present, the electron will then follow a current from n to p through that circuit. Lastly, the electron recombines with the holes in the p-type material.

The external circuit on a solar panel consists of a layer of aluminium on the back of the panel, and aluminium "fingers" on top, which are electronic contacts. The fingers are usually thin in order to avoid shadow, but just enough to conduct current.

The two main types of Si solar cells are mono- and multi- crystalline. As the names imply, the mono-crystalline consists of one crystal, whereas the multi-crystalline consist of several smaller crystals. The main differences in these types are the efficiency and production costs. The efficiency in a mono-crystalline solar cell is 18-24% and is the more costly to produce of the two. Multi-crystalline is cheaper but has an efficiency of 16-18%. Efficiency, in this case, is the fraction or percentage of the energy in the solar radiation that is converted to electrical energy.

Photovoltaic circuit properties

A photovoltaic cell can be seen as a power source, parallel connected with a diode with a pn-junction, see figure 7. The resistances R_P and R_S are internal resistances within the cell. R_P, called shunt resistance, should be as high as possible to diminish the potential loss of power. R_S is a parasite resistance, which should be as low as possible. R represents the external load the cell is connected to. Power through the diode, I_D is given in the equation 8,

$$I_D = I_0 \left(e^{\left(\frac{qU}{k_B T}\right)} - 1 \right) \qquad (8)$$

where I_0 is saturation current for the diode. U is the potential over the PV-cell, q is the elementary charge, k_B is Boltzmann's constant and T is the temperature of the photovoltaic cell.
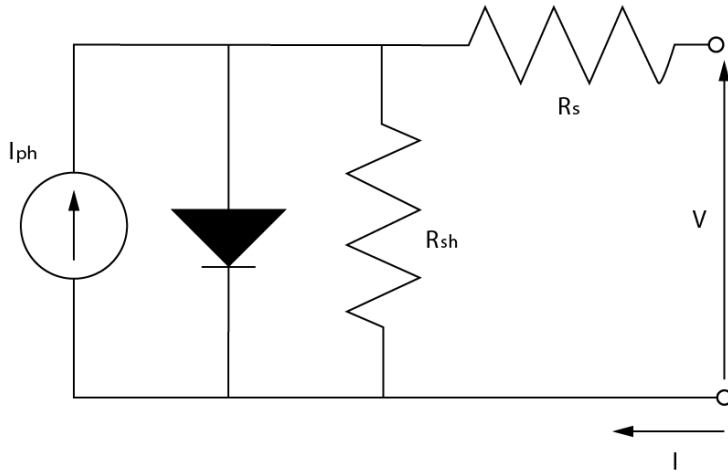
Figure 7: Equivalent circuit of a PV-cell

The fundamental photovoltaic equation gives the power out from the cell, I, and is given by equation 9:

$$I = I_L + I_0 \left(e^{\left(\frac{qU}{k_B T} \right)} \right) - 1 \qquad (9)$$

I_L is the power generated by the incoming photons.

The short-circuit power, I_{SC}, is the power that can be measured in the circuit when the load R is zero. Ideally this should equal I_L.

The open-circuit-voltage, V_{OC} is measured by the open connection points in figure 7. Then the power I equals zero. The expression V_{OC} is given in equation 10. I_L replaces I_{SC} and is a simplification based on $I_{SC} >> I_0$.

$$V_{OC} = \frac{k_B t}{q} \ln \frac{I_{SC}}{I_0} \qquad (10)$$

While the open-circuit power and the short-circuiting power cannot occur at the same time, the possible power-circuit combinations are given in a IV-curve. IV-curves can be given for only one PV-cell and for combinations of several cells.

The power out from a PV-cell is given by the product of the current and voltage, as shown in equation 11, and is always less than the product of the short circuit current and the open circuit voltage, because these cannot occur at the same time.

$$P_{cell} = IV \qquad (11)$$

18

The maximal power from a solar cell occurs when the following criteria is met,

$$dP_{cell} = IdV + VdI = 0 \qquad (12)$$

and the maximal power is then given by 11.

$$P_{max} = I_{mp}V_{mp} \qquad (13)$$

The efficiency of a solar call is measured by how much the product of I_{mp} and V_{mp} fills the IV curve, which is often referred to as the fill factor, represented by the symbol FF,

$$FF = \frac{P_{max}}{I_{sc}V_{oc}} = \frac{I_{mp}V_{mp}}{I_{sc}V_{oc}} \qquad (14)$$

The fill factor also depends on the spectrum of the radiance, the resistivity losses in the cell, and the load connected to the cell.

The fundamental photovoltaic equation gives the power out from the cell, I, and is given by equation 15:

$$I = I_L + I_0\left(e^{\left(\frac{qU}{k_BT}\right)}\right) - 1 \qquad (15)$$

I_L is the power generated by the incoming photons.

The short-circuit power, I_{SC}, is the power that can be measured in the circuit when the load R is zero. Ideally this should equal I_L.

The maximal power from a solar cell occurs when the following criteria is met,

$$dP_{cell} = IdV + VdI = 0 \qquad (16)$$

and the maximal power is then given by 17.

$$P_{max} = I_{mp}V_{mp} \qquad (17)$$

The efficiency of a solar call is measured by how much the product of I_{mp} and V_{mp} fills the IV curve, which is often referred to as the fill factor, represented by the symbol FF,

$$FF = \frac{P_{max}}{I_{sc}V_{oc}} = \frac{I_{mp}V_{mp}}{I_{sc}V_{oc}} \qquad (18)$$

The fill factor also depends on the spectrum of the radiance, the resistivity losses in the cell, and the load connected to the cell.

PV-modules

PV-modules consist of several solar cells. One cell can generate 0,6 V on its own, and connected as a series, up to 57 V. Between 36 and 96 cells are typically connected, which can reach voltage levels from 21-57 V. One cell is typically a square with lengths of 12-16 cm and has a thickness of approximately 0,2 mm. A matrix of modules is formed when PV-modules are connected in parallel fashion, and PV-modules are referred to as a string or array of modules when they are connected in series.

STC and NOCT – test conditions for solar panels

When PV-cells are tested they are exposed to standard test conditions (STC) and nominal operating cell temperature (NOCT). The parameters of STC are as follows,

Irradiation $1000W/m^2$

PV-cell temperature 25 ⁰C

Air Mass 1,5

but these conditions rarely occur outside test sites. NOCT parameters are defined as,

Irradiation $800 W/m^2$

Air temperature 20 ⁰C

Wind speed 1 m/s

The main difference between STC and NOCT is that the cell temperature is defined in the STC method. During NOCT testing, the average temperature of the PV-cells is 48 ⁰C (Luque and Hegedus, 2011).

A PV-module is rated after its power is produced under standard testing conditions (STC). The power it is able to produce under these conditions is called the peak power, W_P. W_P represents nominal conditions, NOCT, usually 70-80% of power produced during STC (Haberlin, 2012).

The effects of shadowing

Shadow falling on a PV-module is a problem. Current from the entire PV-module is affected when one cell is completely or partly shadowed. Trees, buildings, or other objects can cause shadowing of the PV-unit, as well as snow and leaves covering the cells. The reduction of the current from a cell is proportional with the part of the cell that is shadowed. Because the photovoltaic cells are connected in series to create a module, a reduction in one cell will result in a power reduction in the complete module. When in addition the modules are connected in series in a chain, the whole chain will have a reduced production on power.

When one cell has low production of power, that reduces the production in the remaining cells, the cells that are not shadowed produce extra high voltage. All the power generated in the cells that are not shadowed will be deposited in the shadowed cell, if it is in any way defect. Most photovoltaic cell have some sort of defect of some size. This is not ideal - it results in massive heating of the particular cell, so called hot-spot-heating, which can result in glass cracking, metal melting, and reduced capacity of the cell.

Installing a by-pass diode can reduce the effect of shadowing. The passage diode is connected in parallel with a certain number of cells and is in practice an open circuit when all photovoltaic cell functions optimally. If a cell is exposed for shadowing the diode will start to conduct power. This limits the power of the shaded cell, and with that the given effect. It is too expensive to install a diode per cell, therefore it is common to use two diodes per module of 36 photovoltaic cells (Ramabadran and Mathur, 2009).

Battery technology

Batteries store chemical energy and can convert this energy to electrical energy when there is a demand. The electrochemical reactions that occur in the battery cells cycle between discharge and charging currents from 1 to 100 A. Their capacity and voltage depend on which material the components consist of and the battery cell configuration. Theory from this section is based on Renewable Energy Resources chapter 15 (Twidell and Weir, 2015).

Battery cells

In a battery cell, two electrodes are immersed in an electrolyte. The electrodes are usually of different materials and in each of these a half cell reaction occurs.

Lead acid batteries

In electrochemical cells two electrode plates are immersed in a conducting solution, figure 8. This particular one has electrodes shaped as a grid, holding pastes of lead and lead dioxide. To increase the surface area the pastes are made from powder, which gives it a spongy form. Electrodes with a tube form are mechanically stronger, and they are more resistant to shedding, and are therefore suitable for deep discharge. The electrolyte, which is of sulphuric acid, ionises as shown in the following chemical equation

$$H_2SO_4 \rightarrow H^+ + HSO_4^- \qquad\qquad (19)$$

The chemical equation that represents the reaction at the negative electrode during discharge is

$$Pb + HSO_4^- \rightarrow PbSO_4 + H^+ + 2e^- \qquad (20)$$
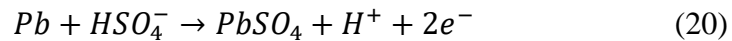
$PbSO_4$ crystals are formed when Pb is oxidized to Pb_2^+. Mechanical expansion is caused when smaller density sulphates takes the place of Pb paste in the plate because of their larger molecular form.

Liberated electrodes contribute to the reaction by travelling through the external circuit to the positive electrode contributing to the following equation

$$PbO_2 + HSO_4^- + 3H^+ + 2e^- \rightarrow PbSO_4 + 2H_2O \qquad (21)$$
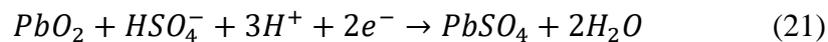
In this electrode $PbSO_4$ replaces the PbO_2, but the electrical current through the solution is carried by H^+ and HSO_4^- ions from the sulphuric acid electrolyte, which also plays a role in the plate reactions.

Transportable «gelled» cells are safer too use and transport because the electrolyte is immobilised in pyrogenic silica, with fibrous glass mat separators, which gives open gas paths for the release of hydrogen and oxygen in overcharge, and therefore there is no danger of spilling corrosive sulphuric acid. This makes them more expensive, but in return they are maintenance free.
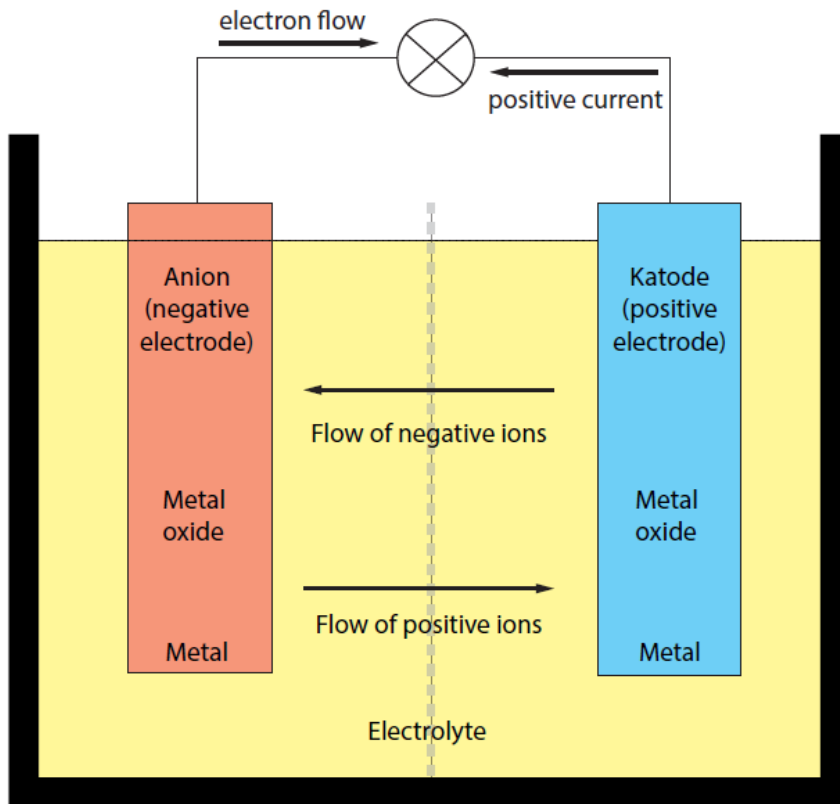
Figure 8: Lead acid battey cell

The theoretical energy density, W_m, can be calculated from the reaction equations and the corresponding standard electrode potentials,

$$W_m = \frac{ne^- * V_e}{m} \qquad (22)$$

where n is the number of electrons, e^- is the electron charge, V_e is the electrode potential and m is the mass of the active ingredients in the battery cell.

High quality batteries have a 25% energy density of the theoretical value, while most commercial batteries only have 15% of the value. There are two main reasons why the battery may fail to reach its full potential. Twiddle and Weir (2015) describe the main reasons for this discrepancy. First, parts of the batter are composed of non-active materials, such as the case and the water where acid is dissolved. Thus, the mass of the entire battery exceeds the mass of the active ingredients, which means the energy density based on the mass of the whole battery is less than the theoretical value based on the active mass alone. Secondly, Twiddle and Weir (2015) go on to explain that the reactions which take place inside of a battery must not be entirely completed. Most types of batteries only discharge about half of the potential stored energy, because a battery must have an electrode and an electrolyte which are adequate and

complete discharge would diminish the battery's ability to operate. However, Twiddle and Weir (2015) go on to explain that some batteries are designed to allow a "deep discharge" beyond 50%.

In practice, batteries have additional limitations. For example, after some cycles the plate material and some $PbSO_4$ form crystals in the electrolyte which fall to the bottom of the cell, potential decreasing the electrode. The consequence of completely emptying the battery is that the battery loses active ions and electrons, which could result in making it impossible to recharge. The crystals that fall to the bottom can also function as a conductor, causing the battery to self-discharge or short-circuiting the electrodes.

Generous space in the cell can prevent short-circuiting of the electrodes, which is important for storage batteries. This is essential for the power supply system of the Thorvald robot.

To ensure the battery lifetime, it is crucial to avoid excessive and frequent discharge.

Discharge characteristics of a battery usually show at which constant current a battery over 20 hours where 100% of the nominal energy stored is used. For a typical car lead-acid battery, with a nominal capacity of $Q_{20} = 100Ah$, where Q_{20} represents the battery's capacity when discharged with a constant current over 20h, the voltage per cell drops from 2.07V to 1.97V as the first 60% of the energy is used and then drops sharper from 1.97V to 1.8V for the remaining 40%. When the battery is discharged at higher currents, thus higher speed, less of the nominal energy is used during the discharge. This is because the reactants in equation 20 diffuse into contact with each other at a certain rate, which limits the reactions at the electrode, due to the reaction products rapidly accumulating and blocking the contact.

Additionally, battery operation is impacted by the depth of discharge (DOD), the current, and the temperature at which the battery is discharged. Batteries with a shallow DOD will need a higher capacity to provide energy for a certain demand than a battery with a deeper DOD. If batteries are discharged further than the DOD, then the number of possible charge and discharge cycles and the battery's lifetime are reduced. The available capacity for each cycle is called state of charge (SOC).

$$SOC = 100 - DOC$$

SOC and DOD, in this equation, are the percentage of capacity.

Available energy in a battery can be calculated by multiplying the capacity with the nominal battery voltage.

$$E = C \cdot V$$

Here, E represents the available energy, C represent the battery capacity, and V represents the open circuit voltage.

Series and parallel battery configurations

Some batteries come as a single cell and some come as a package with multiple cells connected. Connected cells can be configured in either series, parallel, or a combination of these, to achieve a desired voltage and capacity. The total voltage at the terminals of a battery package is the sum of the potential of each cell connected in series, and higher capacity is attained by parallel connected cells. Depending on the number of cells in series and parallel, configurations are referred to as *n*s*m*p, where *n* represent number of cells in series and *m* represents parallel.

Electrical components

In a PV power production system, there are more components than just the PV-cells. The PV-cells should be producing at maximum power. To ensure maximum production, one can use a controller or the battery to ensure that *I* and *V* follow the maximum power line, which will be unbalanced with variations in irradiance and load. By using the battery to control that the power line is followed, the voltage of the array of PV-modules is matched to the nominal battery voltage, and the IV load curve for the battery is matched to the maximum power line of the arrays. Another way this could be accomplished is by incorporating a sophisticated controller into the system.

Controller

A controller optimizes the battery's rate of charge and can also include a maximum peak tracker (MPPT) for PV modules. For reliable operation, the controller provides specified maximum rates of charge and depths of discharge. The controller regulates the current and voltage of the PV array by separating it from the required voltage by the load. In this manner, the controller improves the lifetime of both the PV cells and the battery.

Inverters

When using PV power to operate AC appliances, an inverter is required. An inverter transforms DC to AC, by inverting the DC currents direction many times per second to reach the desired AC frequency. DC sources often come with low voltages compared to the required AC appliance voltage. Thus, inverters come with a built-in transformer to achieve this voltage. The performance of an inverter is one of multiple criteria which are measured by how closely the AC output resembles a sinusoidal wave. A cheap and simple inverter can produce a square wave, while an expensive inverter can produce a wave almost indistinguishable sine wave. Efficiency, size, tolerance with respect to varying input, and reliability are other parameters that determine the performance and differentiates inverters from one another. The efficiency of inverters ranges from 60% to 96% (von Meier, 2006).

Three inverters can be considered for installation when using a PV power system including the central inverter, string inverter, or module inverter.

In cases where matrices of PV modules are installed, it is common to use a central inverter. In this case, only one inverter is used for an entire system which reduces costs. Yet, this configuration demands more cables, which can increase losses due to the resistivity in conductors. Additionally, the current and power delivered by the entire system will be affected by partial shadowing on only one of the modules.

A string inverter inverts current from arrays of modules one by one. If there are multiple strings, the number of inverters will increase as well. This makes for higher costs. However, this configuration allows for less cable usage, which reduces losses. Moreover, if one of the modules are partly shadowed, it will only affect the string involved, and not the entire system.

Module inverters are inverters for each unit in the system. If one module experiences shadowing then it will only affect this one module, and not the entire system. However, these modules operate at lower voltage and have a lower efficiency than central and string inverters. These should, therefore, be used mainly in cases where shadowing is a large problem.

One of the oldest inverters simply changed the direction of voltage and current 120 times per second, by using a rapidly switching electronic circuit. This created a square-wave with the frequency of 60 Hz. However, when this was used to power motors, the energy in the edges of the square was unable to be transformed to torque. Instead, the motor windings were heated. It can also cause buzzing in electronics, such as audio equipment.

Another sine wave generated using the same technique is the modified sine wave. The difference here is that the voltage and current is kept at zero for a short period of time before reversing the direction. An third method is a method that increases the current initially and chops off the output with short intervals. Source: Electric power systems – a conceptual introduction, Alexandra von Meier, Published by John Wiley and Sons, New Jersey 2006.

Strawberry production systems

Open field production

Strawberries are traditionally grown on the ground, which is also known as open field production. This method has several issues, such as botrytis and anthracnose, which many commercial strawberries are prone to, in addition to pests and snails. Harvesting strawberries is hard work, as the pickers must kneel when they are picking the berries. This makes strawberry harvesting more time consuming than necessary, as the working position is not ideal.

Table top production

Another way of producing strawberries is to lift the plants off the ground, which is referred to as table top production. This method has several advantages. There are less problems with snails and pests (Pertot et al., 2008), and the harvesting is much more efficient and comfortable for the worker. Table top production usually takes place in a polytunnel, where the climate and temperature can be somewhat controlled.

In 1998, a farm in England was one of the first to try producing strawberries with a table top production method. Today, electrically operated tunnel doors are used to maintain an optimum growing environment for the plants by automatically opening and closing the tunnels according to temperature and humidity. Simen Myhrene, a strawberries producer, explains that the tunnel provides an increased predictable climate, which is essential for the production of berries and fruits in Norway (Myhrene). In addition to keeping the fruits dry, by protecting them from weather, and making them more resilient to storage, the tunnel also allows for earlier harvesting of the crops. However, table top production of strawberries still poses a few challenges.

UV-treatment against mildew

While table top production is not as prone to botrytis as open field production, the strawberries are more prone to powdery mildew in tunnels, leading to an increased use of chemicals, up to 12 treatments for each growing cycle (Xiao et al., 2001). The health and environmental impact of chemicals, as well as the growing pesticide resistances, requires new alternatives that can be implemented in an integrated pest management (IPM) strategy. Studies in greenhouses at NMBU and NIBIO have shown that UV-B radiations can reduce the severity of powdery mildew by up to 90% without affecting the plant growth (Gadoury et al., 2013). When UV-treatment is applied during the night, it destroys the mutagenic in the mildew, and the mutagenic damages cannot be repaired, as they can be during the day.

Additionally, green house spider mites are also a problem when strawberry production is moved in-house (Xiao et al., 2001). Trials have shown that UV-treatment destroys the eggs and immature stages of mites. However, beneficial insects are the predominant way to get rid of the mites (Easterbrook, 1992). Thus, to make the UV-treatment eligible for practical use, it is important that it is combined with the use of beneficial insects. According to Nina Svae there is "*little knowledge regarding how the low dose of UV-B against powdery mildew will affect the beneficial insects that are used*"(Fløistad, 2016). Johansen also explains that trials will provide new and important information regarding whether UV-B can be used in combination with beneficial insects in the biological control of mildew.

The Thorvald robot in the fight against mildew

UV-B is applied from special fluorescent lights mounted on moving equipment – the Thorvald robot. The robot carries the UV-B equipment along the tables of strawberries during the night. The robot finds its own way, and treats the plants every third night. Figure 9 shows the Thorvald robot in a polytunnel executing UV-treatment of strawberries in table top beds.

Figure 9: Polytunnel, Available at https://sagarobotics.com/pages/light-treatment (read: 05.05.2020)

Thorvald Robot

The Thorvald Robot is a modular robot which can be adapted for different uses and applications. While the frame and battery package of each robot is similar, different application tools can be mounted on the robot for the completion of different tasks (Grimstad and From, 2017).

Battery package

The robots considered in this thesis are equipped with two lithium-ion battery packages. Rated capacity for the cells in the battery is 3000mAh with a nominal voltage of 3,6V. For the battery package the rated capacity is 70Ah and the factory voltage is 48-50V. The combination method is 13S24P.

System requirements

Requirements for the system are listed below

- Charging station must not be connected to the power grid
- Charging station should be carbon neutral

Energy calculations

In order to find the size of the solar panels that supply energy in this system, energy calculations have been carried out. First, the system is comprised of the following components: the solar panel(s), the maximum power point tracker, the battery, the inverter, and the induction charger (figure 10). Each of these components has a respective efficiency, which has been used to calculate the minimum size needed for the battery bank and the PV-modules. An overview of the system is shown in the figure below.
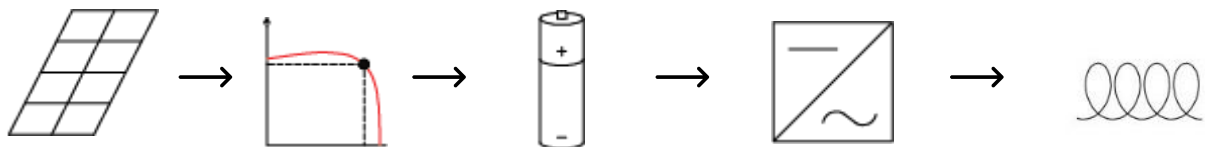

Figure 10: PV-module, Maximum power point tracker, battery, inverter and induction charger

To calculate the energy flows from each component the following equations were used, and efficiencies were found in theory or product specifications:

$$\mu_C = \frac{E_C}{E_I}$$

$$\mu_I = \frac{E_I}{E_B}$$

$$\mu_B = \frac{E_B}{E_{MPPT}}$$

$$\mu_{MPPT} = \frac{E_{MPPT}}{E_{PV}}$$

$$\mu_{PV} = \frac{E_{IR}}{E_{PV}}$$

Component	Symbol	Efficiency	Value	Icon
PV-module	PV	$\mu_{PV} = \dfrac{E_{IR}}{E_{PV}}$	0.15	
Maximum power point tracker	MPPT	$\mu_{MPPT} = \dfrac{E_{MPPT}}{E_{PV}}$	1.0	
Battery	B	$\mu_B = \dfrac{E_B}{E_{MPPT}}$	0.90	
Inverter	I	$\mu_I = \dfrac{E_I}{E_B}$	0.96	
Induction charger	C	$\mu_C = \dfrac{E_C}{E_I}$	0.90	
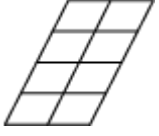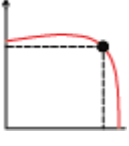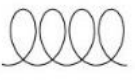
The equations show the efficiency of the components in the system, and *E* represents the energy that either enters or goes out of the component (Table 1). In many of these cases, the efficiency of the component is known, which can then be used to estimate the size of the battery bank and the PV modules. The total efficiency of the system is found by

$$\mu_{TOT} = \mu_{PV} \times \mu_{MPPT} \times \mu_B \times \mu_I \times \mu_C$$

which is equal to $\mu_{TOT} = 0.117$ or 11,7%.

Farm data

Location of the farm, topography, size of the farm and area of the field is presented in table 2.

Table 2: Farm data

Location	Coxheath, England
Coordinate position	51.2, 0.499
Altitude	130 m
Field area	30 000 m²
Shadowing objects	None

Topography

Kent, South East, England, United Kingdom (51.24748 0.71051)
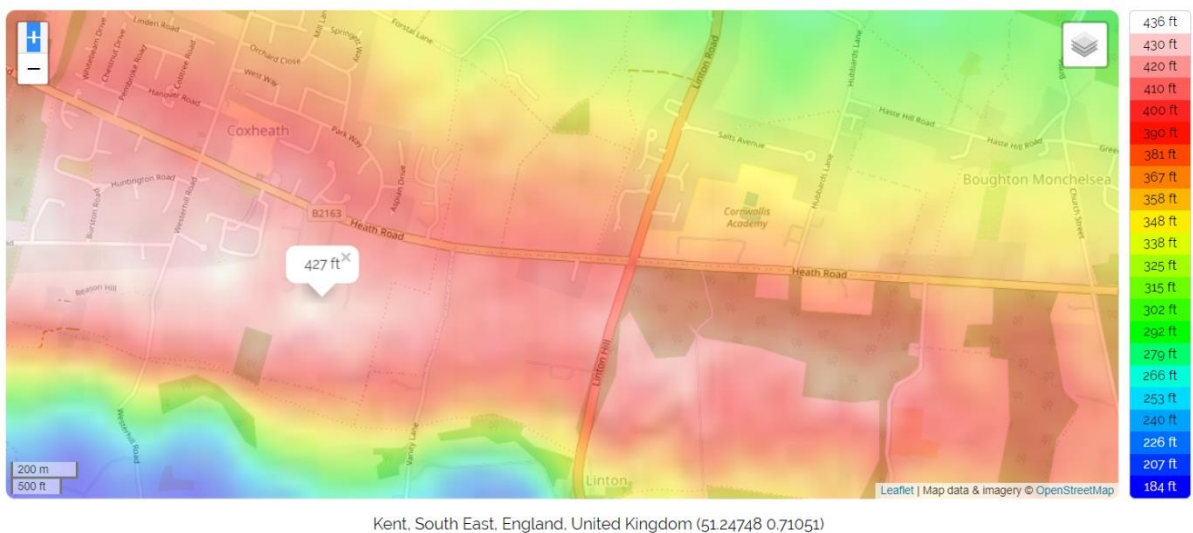
Figure 11: Topography of Kent

Figure 11 shows the topography of Kent, and the white bubble marks the position of the farm. The scale on the right side of the figure shows that altitude ranges from 184 ft – 436 ft, which is the equivalent of 56 m – 133 m. The farm position is located approximately on top of the hill, and therefore there are no shadowing objects due to the topography of the location. If there had been high mountains nearby, this would have affected the amount of irradiance at the location. The map is supplied by Leaflet, which is an open source JavaScript library for interactive maps (Agafonkin, 2019).

Planting, UV-treatment and picking of strawberries

UV-treatment usually starts two weeks after planting, and approximately 45 day prior to

picking the berries. UV-treatment using the Thorvald robots started march 2nd this year according to personal communication with Lars Grimstad (Grimstad, 2020).

Robot energy consumption

Table 3 shows data from two robots in the field of the actual farm. The two robots were able to treat strawberries with UV-light in 5.78 h and 5.53 h, each with battery consumption of 75% and 72%, respectively.

Table 3: Battery data for UV-bots

Robot	Scenario	Date	Operation time	Total distance	Average speed	Battery consumption
Thorvald-23	UV-treatment	16.03.2020	5h 46.5min	9096.57m	0.44 m/s	75 %
Thorvald-25	UV-treatment	16.03.2020	5h 31.6min	9231.28m	0.46 m/s	72 %

The robots are equipped with two battery packages and each have a capacity of 70 Ah and voltage of 48-50 V, which make up a total capacity of 3500 Wh. The total energy capacity of each robot is then 7000 Wh.

The energy consumption of the harvester has not been measured. For this thesis it is estimated that the energy consumption of the harvester is the same as for the UV-bots.

Single robot

The data above has been used to create some minimum values for a single robot and what it is able to do.

One robot can cover 1.5 hectares with a battery consumption of 75% of the battery's capacity. Energy consumption for one robot covering 1.5 hectares is 0.75*7000 Wh = 5250 Wh.

Energy consumption per hectare, per robot, per treatment is 5250 Wh/1.5 hectares = 3500 Wh/hectar.

Robot fleet

A robot fleet, consisting of two UV-bots and one strawberry picker, has the energy demand profile for one week as shown below. This is currently the energy demand profile at the farm in Coxheath, England.
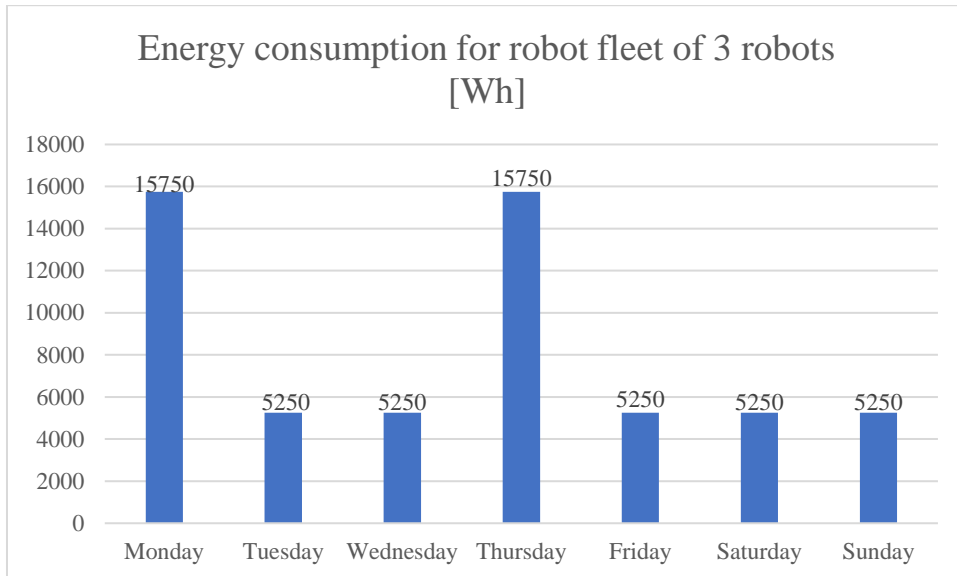

Figure 12: Energy consumption for a week

From figure 12, one can see that from Tuesday to Thursday the total energy demand is 15750 Wh + 2*5250 Wh = 26250 Wh by three days. This gives a rate of 26250 Wh/3days = 8750 Wh/day. This represents the daily energy that must be produced, without losses, to meet the energy peaks twice a week. The peak of 15750 Wh represents the SOC of the stationary battery, without losses, meaning the true SOC will have to be greater than this.

Battery bank

The battery bank must maintain the amount of energy needed during the peak energy demand of the robots. This includes the energy loss which occurs when the energy is transmitted from the battery, through the inverter and induction charger. To determine the required capacity of the battery bank, the system losses need to be calculated.

In order to find the battery capacity, the SOC must be determined first, as batteries vary in their DOD. Two types of batteries which will be presented here are Li-ion and lead-acid batteries.

Li-ion batteries are more sensitive to being over-discharged, as this can cause permanent damage. As the goal of the system is to be completely autonomous, a Li-ion battery can be risky. However, Li-ion batteries come with battery management systems (BMS), to mitigate

this risk. In addition, Li-ion batteries represent a strong choice because of their ability to provide stable voltage, or the same voltage, during the entire discharge period, until there is a sudden drop in voltage, when approximately 20% of the battery capacity is left. In contrast, a lead-acid battery cannot deliver the same voltage level as it discharges, although it can withstand a deep discharge better than a Li-ion battery.

Another difference between the two types of batteries is that the SOC of lead-acid batteries is typically 50% and Li-ion is 80% of the battery capacity. Li-ion batteries can endure more charge/discharge cycles, and therefore, have a longer battery lifetime than lead-acid batteries. However, a Li-ion battery can be permanently damaged if discharged further than the DOD.

The energy density of a Li-ion battery is higher than a lead-acid battery. This means that a Li-ion battery contains more energy than a lead-acid battery per kilo. This is an advantage for the system designed in this project, because the system will be placed in a mobile container, which should ideally be held at lowest weight possible. A disadvantage of the Li-ion battery is that it costs more.

Battery bank SOC size is found by using the following equation

$$SOC = 15{,}75 kWh \times (1 + (1 - \mu_B) + (1 - \mu_I) + (1 - \mu_C))$$
$$= 15{,}75 kWh(1 + 0{,}1 + 0{,}04 + 0{,}1) = 19{,}53 kWh$$

SOC accounts for 80% of the total battery capacity, C_B, which leads to a total battery capacity of

$$C_B = \frac{SOC}{0{,}80} = \frac{19{,}53 kWh}{0{,}80} = 24{,}4 kWh$$

Solar energy

Data downloaded from PVGIS using the PV-SARAH calculation method.

Irradiance
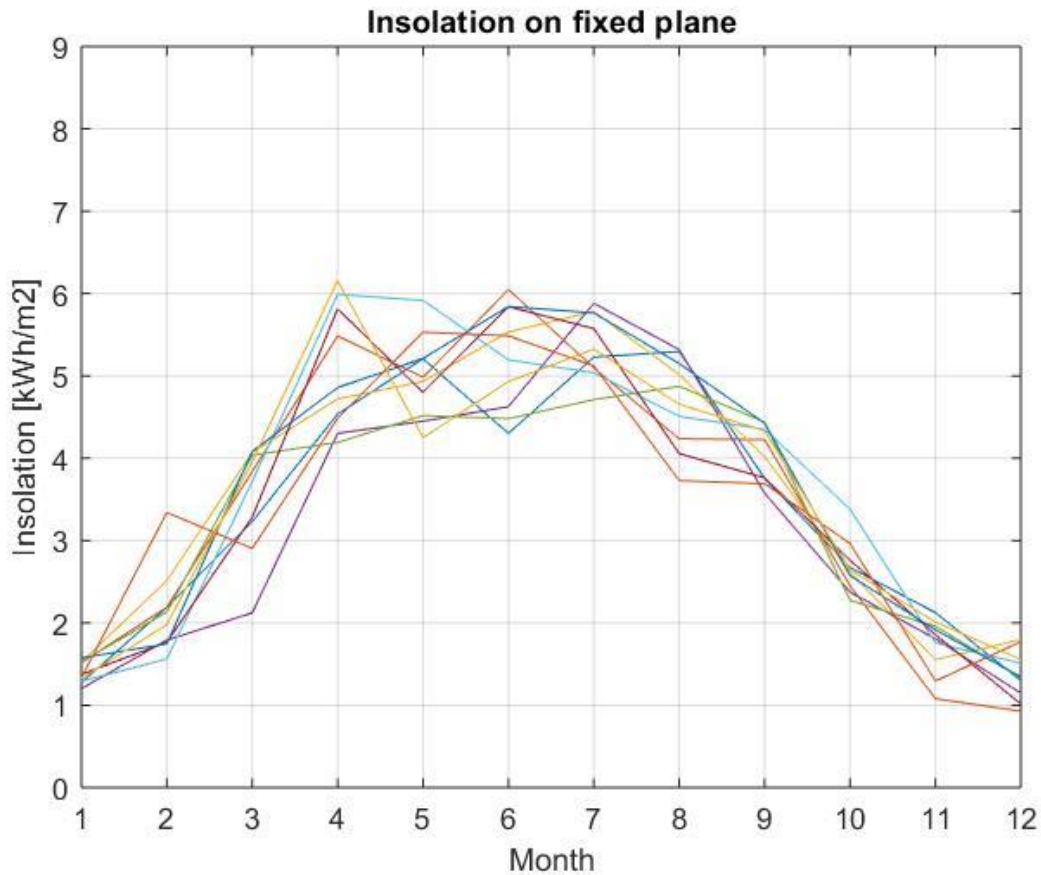
Figure 13: Insolation, fixed plane

Figure 13 shows the irradiance from the sun on a fixed plane, month by month, from 2007 to 2016. The numbers on the x-axis represent each month of the year starting with January. Each of the lines represents the insolation, month by month, for a single year. As seen in the figure, in months 4-7, April through July, the insolation varies very little from month to month. However, there are variations from year to year for each of the months. For example, the average insolation in April varies from just above 4 kWh/m^2 to just above 6 kWh/m^2.
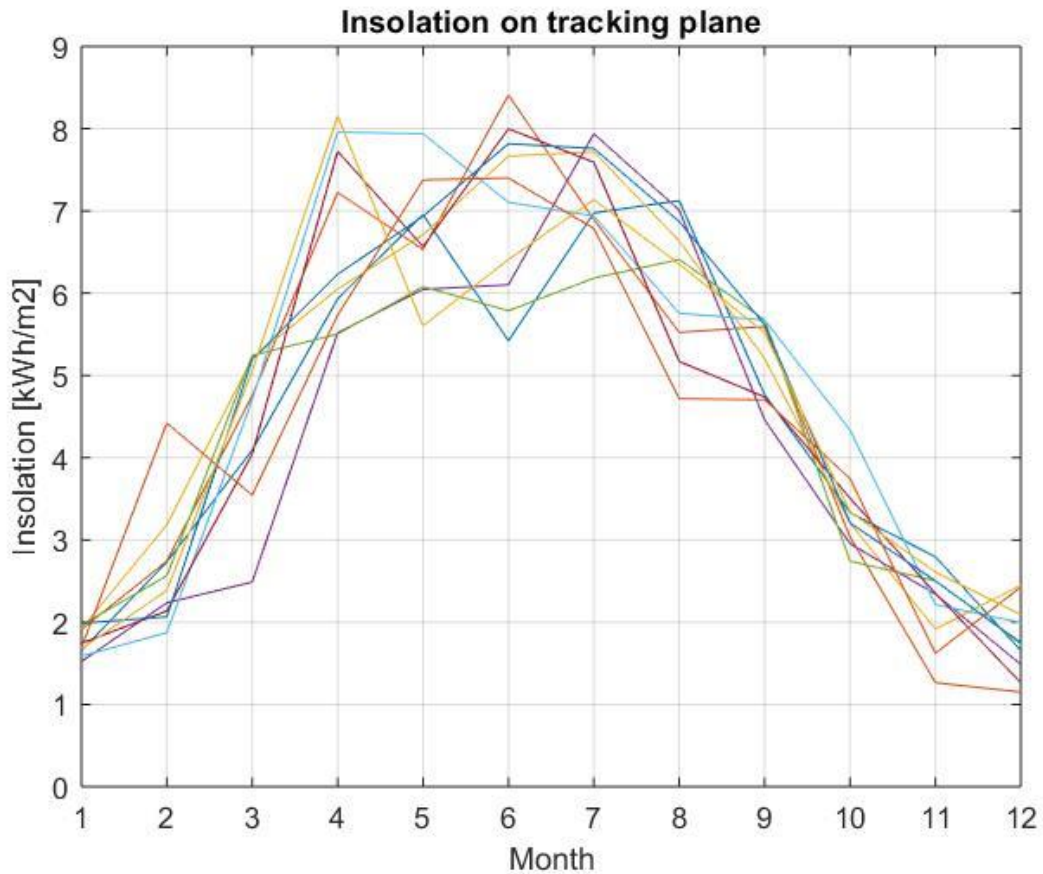
Figure 14: Insolation, tracking plane

Figure 14 shows insolation on a tracking plane, month by month, from 2007 to 2016. All of the years follow the same trend, but there are some variations from year to year for each of the months. One month of particular interest is month 6, June, which varies between approximately 5,5 kWh/m^2 and almost 8,5 kWh/m^2. These variations do not correspond to variations for the same month for a fixed plane.
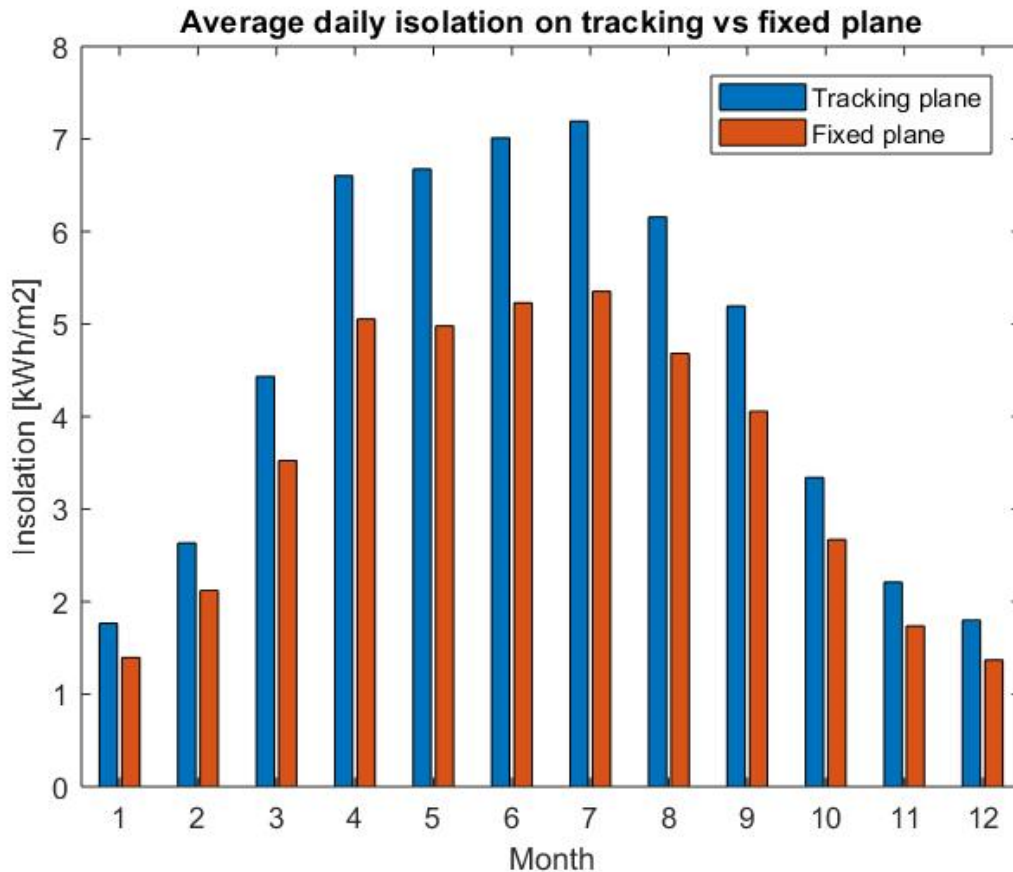
Figure 15

Figure 15 shows the average daily insolation on a tracking plane and a fixed plane. This figure demonstrates the difference in insolation on tracking versus a fixed plane.

The most critical month

A critical point for this study is when the radiation is low, but energy demand is high. However, the average daily insolation from April to August appears to vary very little. If the farmers are able to stretch the strawberry season until September, where the daily average insolation seems to drop, the system dimensions should calculated to supply the robots with energy, even on the days with the least irradiation from the sun.

Table 4 shows the average daily insolation and the standard deviation for each month during the year and corresponds with the bar diagram above. The standard deviation is included to find the uncertainty in how much insolation there is during the day, which implies which month has the highest variance. The data from table 4 shows that April is the month with the highest standard deviation, and therefore, the month with the highest variance and variation in insolation.

Table 4

	Daily insolation [kWh/m2]			
	Tracking plane		Fixed plane	
	Average	Std	Average	Std
January	1.395	0.130	1.766	0.167
February	2.120	0.512	2.634	0.737
March	3.524	0.640	4.433	0.897
April	5.054	0.739	6.603	1.050
May	4.980	0.511	6.674	0.681
June	5.228	0.620	7.011	1.021
July	5.352	0.384	7.192	0.548
August	4.683	0.546	6.157	0.825
September	4.057	0.337	5.195	0.480
October	2.671	0.317	3.340	0.449
November	1.736	0.332	2.211	0.475
December	1.370	0.294	1.800	0.444

Due to the high variation in April, this month has been studied further. Figure 16 shows the insolation in April from 2007 - 2016.
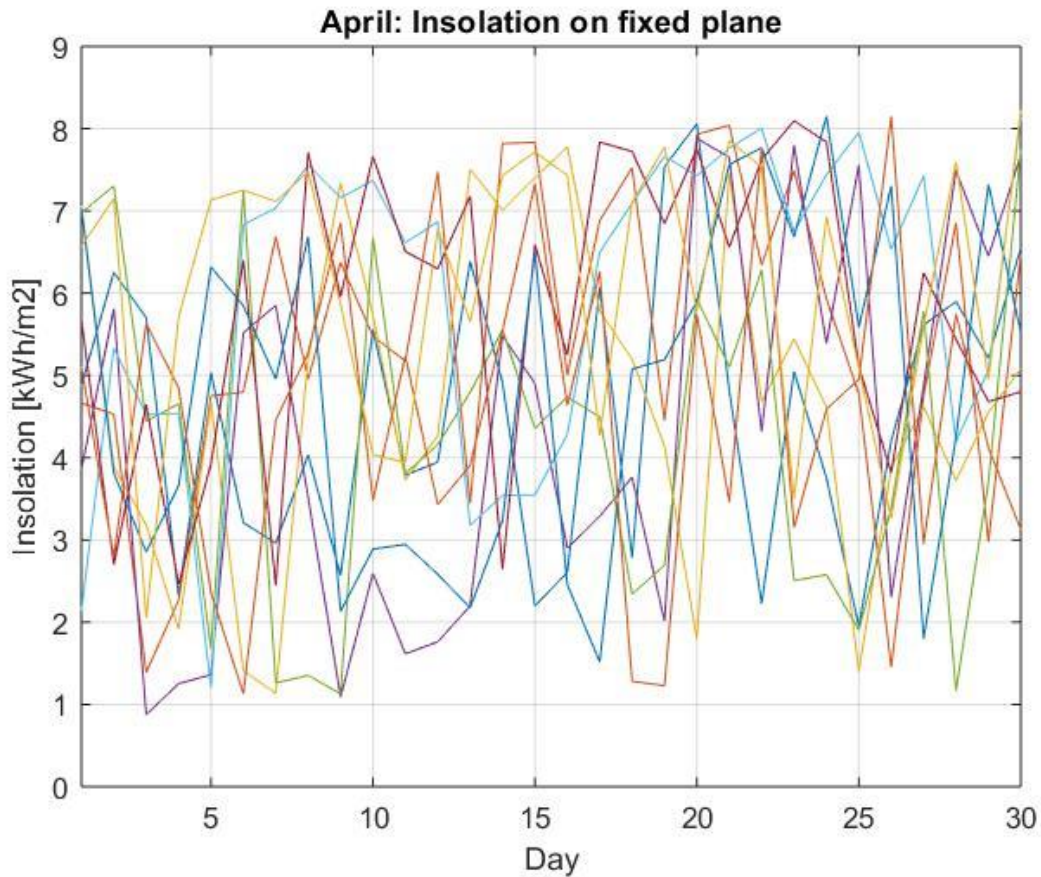
In April, there are large variations in insolation from day to day (Figure 15). Thus, while there can be days with very low insolation in April, this does not seem to occur several days in a row.

When calculating the expected irradiance from the sun, it is crucial to consider the days with little incoming irradiation. While the PV-modules must supply sufficient amounts of energy on days with little irradiation, these days should not be weighted too much. The high levels of variation allow for days where radiation higher than average can make up for the lost production on other days.

PV power production

PV-modules must be able to produce sufficient energy in days with little insolation, and also produce the energy that will be lost in the power transmission throughout the other components of the system.

For the PV-cells to charge the batteries, the voltage from the MPPT must be slightly higher than the battery voltage. The MPPT will be able to regulate this in some way, but it is

important that the modules have areas that are large enough to generate the preferred voltage for battery charging. The voltage of the PV-modules can also be controlled by the configuration of the solar modules. Solar modules in series will generate a higher voltage than a parallel configuration. The current from PV-modules in a series configuration is limited to the lowest current that is generated in the "group" of modules. If one of the modules is subjected to partial shadowing, this will affect the power production from the entire installation. Considering the assumptions made for this project, that trees or other shadowing objects of great significance are absent, the optimal configuration for the PV-modules is a series connection. This will ensure a high voltage and charging of the battery.

Table 5 shows the expected energy production from a PV-module with the efficiency of 20% during NOCT which is the equivalent of an efficiency of 75%. The total efficiency then becomes 15%.

Table 5: Expected PV energy production per square metre

	PV energy production [kWh/m^2]	
	Fixed plane	Tracking plane
January	0.209	0.265
February	0.318	0.395
March	0.529	0.665
April	0.758	0.990
May	0.747	1.001
June	0.784	1.052
July	0.803	1.079
August	0.703	0.924
September	0.609	0.779
October	0.401	0.501
November	0.260	0.332
December	0.205	0.270

To produce sufficient amount of energy of 8,75kWh per day, with the total efficiency of 11,7%, the demand for daily insolation is

$$E_{demand,insolation} = \frac{8,75 \; kWh}{0,117} = \; 74,8 \; kWh$$

The area, A, of the solar panels is then calculated by dividing the energy demand by the average daily insolation, and is presented in table 6 for each month

Table 6: Area of PV-cells

	Area [m^2]	
	Fixed plane	Tracking plane
January	357.4	282.4
February	235.1	189.3
March	141.5	112.5
April	98.7	75.5
May	100.1	74.7
June	95.4	71.1
July	93.2	69.3
August	106.5	81.0
September	122.9	96.0
October	186.7	149.3
November	287.2	225.5
December	364.0	276.9

System specification

In order to supply the fleet of robots with energy an area of fixed PV-modules of 100m^2 is necessary, or 75 m^2 with sun tracking PV-modules. Fixed PV-modules should be tilted an angle of 35 degrees and 0 degrees azimuth.

The battery banks necessary total capacity is 24,4kWh with an SOC of 19,53kWh. A Li-ion battery is necessary to reach these conditions.

Discussion

Robot energy consumption

When the battery consumption was calculated, the percentage of battery consumption was multiplied with the battery capacity from the data sheet. On this data sheet, the battery capacity represents the capacity under optimal conditions, which is of particular importance to note. The measurement was performed on March 16th , from 18 o'clock until midnight, when temperatures in South East England can be expected to be much lower than 25⁰ C. As mentioned in the theory section, battery capacity reduces as the temperature drops, creating an uncertainty in the practical application of these calculations. The percentage of battery capacity consumed per treatment might be lower during warmer months, even though the amount of energy is the same for each treatment. This affects the calculations for how many solar panels are needed, to supply the charging station, with great significance. A solution to this problem is to use weather statistics to find the expected temperature of the time period in question, and calculate the expected battery capacity at this temperature, using the information about battery characteristics.

Peak energy demand

The energy peak is calculated by assuming that the two UV-bots execute the UV-light treatment at the same time. If the robots had their designated area to treat and could execute these tasks at different times during the week, this would reduce the peak energy demand with one third and would play a great role for the necessary battery capacity. The PV-modules would have still had to produce the same amount of daily energy, but the requirement for the battery's SOC to be as high as the peak demand could be reduced.

PV power production

PV-cells' efficiency reduces with higher temperatures. It is reasonable to assume that the PV-modues cannot utilize all the insolation during the warmest summer months for power production. However, the insolation is higher in these months and overproduction may occur instead.

In the energy calculations tracking PV-modules has a higher energy production for each of the months. However, sun tracking PV-modules need more maintenance than fixed PV-modules due to moving parts which conflicts with having a system that is low-maintenance.

Conclusion

To supply the fleet of robots, it was found that 100m^2 of fixed PV-modules or 75 m^2 of sun tracking PV-modules, and a battery capacity of 24,4kWh is necessary to meet the set requirements for the charging station.

Further work

A control system for the charging station is not included in this thesis, although a control system could optimize the power usage and production. A control system would ideally be able to communicate with the entire robot fleet and read the robot's battery levels, the robot's next tasks, and the weather forecast. This helps to achieve a system that controls the robot's work intensity, and thus, controls the battery discharge current, according to the estimated energy production due to the weather forecast. While, the control system of the energy distribution is indeed interesting and crucial to the optimization of the charging system, the scope of this thesis is primarily to find the energy demand and the dimensions for power plants that can deliver this demand.

References

AGAFONKIN, V. 2019. *Leaflet* [Online]. Available: https://leafletjs.com/ [Accessed 2020].

EASTERBROOK, M. A. 1992. The possibilities for control of two-spotted spider mite Tetranychus urticae on field-grown strawberries in the UK by predatory mites. *Biocontrol Sci. Technol.,* 2**,** 235-245.

FLØISTAD, E. 2016. *Lyser bort soppsjukdommar om natta* [Online]. Available: https://www.nibio.no/nyheter/lyser-bort-soppsjukdommer-om-natta [Accessed].

GADOURY, D., SUTHAPARAN, A. & STENSVAND, A. 2013. UV-B as a means to control powdery mildew in strawberry. *Nordic Assn. Agric. Sci.*

GRIMSTAD, L. 2020. *RE: Strawberry UV-treatment and picking dates.*

GRIMSTAD, L. & FROM, P. J. 2017. The Thorvald II Agricultural Robotic System. *Robotics,* 6.

HABERLIN, H. 2012. *Photovoltaics: System Design and Practice,* Chichester, United Kingdom, Wiley & Sons.

HUNT, V. D. 1983. *Industrial Robotics Handbook,* New York, Industrial Press Inc.,U.S.

LUQUE, A. & HEGEDUS, S. 2011. *Handbook of Photovoltaic Science and Engineering.*

MYHRENE. *Hagetunnell* [Online]. Available: http://www.myhrene.no/hagetunnel.html [Accessed 19.04.2020].

PERTOT, I., ZASSO, R., AMSALEM, L., BALDESSARI, M., ANGELI, G. & ELAD, Y. 2008. Integrating biocontrol agents in strawberry powdery mildew control strategies in high tunnel growing system. *Crop Prot,* 27**,** 622-631.

RAMABADRAN, R. & MATHUR, D. 2009. Impact of partial shading on solar PV module containing series connected cells. *SHORT PAPER International Journal of Recent Trends in Engineering,* 2.

TWIDELL, J. & WEIR, T. 2015. *Renewable Energy Resources,* New York, Routledge.

VON MEIER, A. 2006. *Electric Power - A Conceptual introduction,* New Jersey.

XIAO, C. L., CHANDLER, C. K., PRICE, J. F., DUVAL, J. R., MERTELY, J. C. & LEGARD, D. E. 2001. Comparison of epidemics of Botrytis fruit rot and powdery mildew of strawberry in large plastic tunnel and field production systems. *Plant Dis.,,* 85**,** 901-909.